Analysis of Time-Evolved Spectroscopic Ellipsometry Data from Patterned Structures for Etching Process Monitoring and Control

W.Kong, H.T.Huang, M.E. Lee, C. Galarza, W. Sun and F. L. Terry, Jr.
Department of Electrical Engineering and Computer Science, University of Michigan, Ann Arbor, MI. 48109-2122

The use of optical metrology, including ellipsometry and reflectometry, has been successful for process monitoring. However, their applications to actual production are limited due to the problems inherent in the analysis of reflected light from patterned structures. In this paper, we examine techniques for the quantitative analysis of data from both highly regular grating structures and from patterns with low local order. We find good quantitative agreement of vector diffraction theory to specular reflection data. It is demonstrated that the shape evolution of spectroscopic ellipsometry data during etching process is useful for in situ analysis of wafer state. We conclude that there is significant promise for the use of specular techniques for in situ monitoring of topography provided that computational speed issues can be improved.

Introduction

Advanced semiconductor process development and control requires high accuracy, high speed, non-invasive wafer topographic monitors. Specular reflected light techniques, including both single wavelength and spectroscopic versions of ellipsometry (1) and reflectometry (2,3), have been used successfully for both etch and growth rate control of vacuum processes on unpatterned substrate. However, applications of these methods in actual production have been very limited due to the problems inherent in monitoring patterned structures. Recently, multi-wavelength ellipsometry utilizing scalar theory has been used to monitor patterned structures (4). However, the scalar approach becomes inaccurate as the investigated feature size goes into sub-micron regime. Scatterometry for ex situ applications by analyzing diffracted intensities vs. angle of incidence (5), or relative intensity of several diffracted orders at a single incident angle (6) has also been reported. However, for *in situ* applications, it is often only possible to obtain specular reflection information at a single angle of incidence. In this paper, we will present results on applications of scalar models and vector diffraction theory to the analysis of spectroscopic ellipsometry (SE) data from patterned structures. Strong potential of specular measurements for topographic monitoring is indicated.

Experiments

Three types of experimental samples were fabricated for SE tests. The first was a set of relief grating etched in (100) orientation single crystal Si wafers. Gratings with nominally equal lines and spaces were fabricated with periods of 2, 4, and 10 μm. They were fabricated by conventional photolithography and etching process. Six wafers were etched to different depths (approximately100 to 600 nm in 100 nm increments) by changing the etching time. We concentrated our analysis efforts on the 500nm deep grating. The other wafers were used to simulate *in situ* data from the etching process. Post-etch cross-section scanning electron microscopy (SEM) was used to evaluate the line structure profile on the 500 nm sample (shown in Figure 1). The lineshapes can be modeled as trapezoidal. There appears to be some concave-down rounding of the bottoms of the grating. This may have some influence on the results of our attempts to fit optical data from these structures.

Figure 1. Cross-sectional view of 4 μm period Si relief grating. We estimate the structure as: period = 3.96 μm, top linewidth= 2.2 μm, depth = 0.5 μm, and wall angle = 73°.

The second set of samples was a set of aSi:H on Cr on glass samples from our flat panel display efforts. The samples contain no array structures within each die. The die are square and have a repeat distance of about 360 μm. Approximately 100 nm of Cr was deposited by magnetron sputtering on Corning 1737F glass substrates. The aSi:H was deposited using a PlasmaTherm Clusterlock 7000 PECVD chamber and then etched using conventional photolithography and selective wet chemical etching.

The third type of samples was a patterned SiO_2 structure on Si. This sample was obtained from the source drain area of a TFT for flat panel displays. The thickness of the SiO_2 is 491.8 nm.

All SE, SR and scattering measurements were performed on a Sopra GESP-5 spectroscopic ellipsometer/photometer system.

Modeling and Simulation

For scalar analysis, we are using the modified Heimann approach (7) of the Lucent group (5). For diffraction

analysis, we are using both commercial grating simulation software (8) which uses the rigorous coupled wave analysis (RCWA) method (9) and our own software which uses a surface integral equation (SIE) method (10). We also developed our own software to examine the speed of convergence and accuracy of RCWA method.

The scalar model assumes that the total reflection coefficient of the structure can be calculated as a complex combination of the individual reflection coefficients from the different uniform thin film regions, i.e.,

$$R_p = \sum_{i=1}^{2} af_i \exp\left(2j\frac{2\pi}{\lambda}\delta_i \cos(\phi_0)\right) R_{p_i} \quad (1)$$

$$R_s = \sum_{i=1}^{2} af_i \exp\left(2j\frac{2\pi}{\lambda}\delta_i \cos(\phi_0)\right) R_{s_i}$$

where R_{p_i} and R_{s_i} are the reflectances in the p and s polarization corresponding to the i-th region. The nonnegative real number af_i is the area fraction of the i-th region. In Eq. (1), δ_i is the thickness of a layer of vacuum added on top of the i-th region to consider the phase lag due to the different heights of the stacks. Now, as usual, the ratio of R_p and R_s determines $\rho = \tan(\Psi)e^{j\Delta}$. The coefficients R_{p_i} and R_{s_i} are well-known nonlinear functions of the thickness of the layers in each stack (11). One of the limitations of this model is that the effect of finite coherence length is not considered. This effect tends to reduce the constructive and destructive interference in the reflected beam. We have developed a first order correction to include this effect in the scalar model. The computational load of the scalar model is equivalent to the requirements of four different models for blanket wafers and is negligible compared with the vector diffraction models.

The RCWA algorithm finds a set of inhomogeneous plane waves which approximate the exact solution of the Maxwell's equation boundary value problem defined by the grating. The set of differential equations is solved with standard difference equation - eigenmatrix methods. Arbitrarily complex grating line profiles are approximated with discrete slices. The number of slices, s, and the number of plane waves (the order of algorithm, N) determines the computation time/wavelength point and simulation precision. A 2(N+1)s x 2(N+1)s matrix problem is created, but can be solved relatively efficiently due to the 4s x 2s block diagonal character of the matrix. For ellipsometry simulations, the complex *s*- and *p*-polarization fields were first computed and the tan(ψ) and cos(Δ) quantities were computed from these fields. In all our RCWA simulations, we used 10 slices to approximate the grating profiles. One limitation of the commercial software is that it will not use point-wise optical refraction indexes. To overcome this difficulty, we fitted silicon's *n* and *k* by a 10^{th} order polynomial (the maximum the software allowed). This introduced about 3% error in the worst region. The order, N, for our simulations was determined on the basis of energy conservation, and was typically in the range of 45-65. Our typical run times were on the order of 2.1-5.4 minutes/wavelength on a 300 MHz Pentium II™ system (so that a 100 wavelength SE simulation for a given structure could take up to 9 hours). Parallel computation can offer great time advantages but was not pursued in this initial effort.

We also developed our own RCWA software to study the convergence and accuracy of the algorithm. We find that the speed of convergence is slower for shorter wavelengths. In our regime of spectrum, the typical convergent order is larger than 50, while the number of slices required for sufficient accuracy is no less than 4.

The SIE algorithm uses a number of surface current filaments placed at the boundary between two media (air and Si in our case). By utilizing the equivalence theorem (a generalization of Huygen's Principle) and a two-dimensional periodic Green's function as a kernel, the diffracted field above and below the Si surface can be convoluted to form a single integral equation. By matching boundary conditions, the continuity of tangential components of both the E and H fields, the amplitude and phase of each surface current filament can be solved. The field of each diffraction mode can then be evaluated by the interference from these secondary filament sources. The typical execution times for this algorithm were 1.3 minutes/wavelength using 16 filament/(wavelength spacing on the grating) on a Sun Ultra Sparc 1 workstation.

In comparison with RCWA, the SIE approach uses fewer unknowns, and thus reduces the size of the variable matrix. Also, the most time-consuming part in the SIE algorithm, the evaluation of the periodic Green's function, must only be calculate once for both s and p polarization. Therefore, this method is much more computationally efficient than RCWA. To date, we have only been successful in applying the SIE model to the normal incidence case.

Experimental Results

For the scalar analysis of the aSi:H/Cr/glass samples, the structure was divided into two thin film regions. We have included a native SiO_2 layer on top of the wafer. In addition, based on SE measurements of unpatterned aSi:H films on these substrates, we have inserted a thin surface roughness layer between the aSi:H and the Cr substrate. The refractive index of this layer was calculated with Bruggeman's effective media approximation using 50% of amorphous silicon and 50% of Cr.

We have measured tan(Ψ) and cos(Δ) at an angle of incidence of 75°. Figure 2 shows the results of fits with this model. The model is in near-perfect agreement with the experimental data for tan(Ψ). Moreover, the area fraction of region 1 obtained by the model is very close to the nominal area fraction deduced from SEM measurements (about 9.3%). However, the scalar model shows an almost constant offset in cos(Δ). This effect is evident in the data

presented by the authors of as well. This difference may be due to diffraction effects even though the pattern repeat distance is very long for these samples.

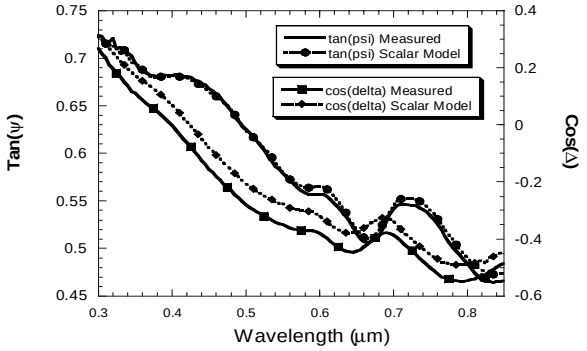

Figure 2. Measured SE data and fit of the scalar model for the aSi:H test structure. Model parameters: region 1- 10.96% (94.52Å SiO2 / 2888.42Å a-Si / 197.09Å roughness / Cr); region 2- 89.04% (8.89Å roughness / Cr).

This scalar model is not always successful due to the finite coherence length effects which reduce the degree of constructive and destructive interference in the reflected beam. A first order correction was used to modify the scalar model. Figure 3 shows the comparison of the performance of the scalar model and its modification when both modes are applied to a patterned structure of SiO2 on Si. It is clear that the modified scalar model is able to capture the features of the measured data better than the original scalar model.

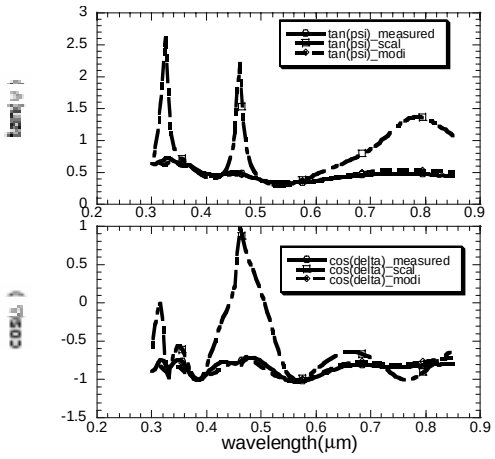

Figure 3. Comparison of the scalar model and modified scalar model for a patterned structure of SiO_2/Si. The thickness of SiO2 is 491.8 nm. The angle of incidence is 64.5°.

On the grating structures, SE data were collected from several dies on the 500 nm depth sample at 75º. Typical data are illustrated in Figure 4. Data were collected both with the plane of incidence normal to the grating and parallel to the grating. As expected, we observed the strongest grating induced structure in the SE data for the case normal to the grating direction. As very long times are required for the RCWA simulation, we concentrated our data analysis efforts on an arbitrarily selected single 4 μm period grating the normal-to-the-grating geometry.

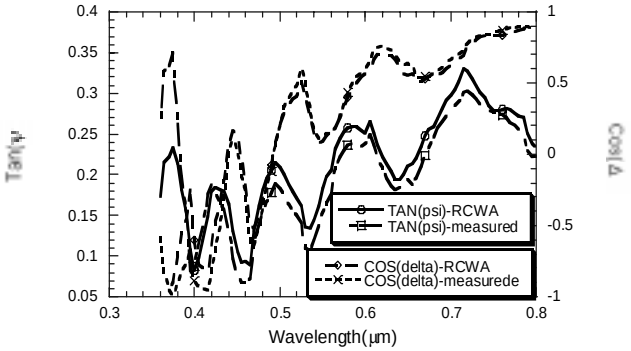

Figure 4. Measured SE data from the 500 nm depth, 4 μm period sample. The plane of incidence was normal to the grating. The RCWA simulation yielded a period of 4.0 μm, a top linewidth of 2.2 μm, a sidewall angle of 72.95º, and a depth of 480 nm.

Our RCWA simulations show several general trends. The positions of peaks and valleys in the oscillations in tan(ψ) and cos(Δ) vs. λ are very sensitive to the period of the grating, while the magnitudes of both ellipsometric parameters were very sensitive to the structure depth. More subtle but still strong structures in the curves are related to the details of the lineshapes. The concave-down rounding may have significant effects on the curve shapes, especially for the longer wavelengths. However, these effects are not mutually orthogonal, so it is not a straightforward exercise to extract the topography information from even these simple test structures. Samples with additional thin film structure would present even stronger challenges.

Therefore, we used a hybrid procedure for finding approximate fits to the grating topography. First, we measured the scattering data to extract the grating period using the grating equation:

$$p \cdot \sin\phi = k \cdot \lambda \qquad (2)$$

where p is the grating period, k is the diffraction order, and ϕ the diffraction angle. We can measure up to 4th order of diffraction, and calculate the period with accuracy in the range of 10 nm. Then we measured both near-normal (6º) s- and p-polarized SR and SE data, and 75º SE data. Simple scale theory allow the thickness to be estimated from ¼ wave interference between waves reflected from the top and bottom of the grating:

$$1/4d = (1/\lambda_{peal} - 1/\lambda_{valley}) \qquad (3)$$

We used this estimate on the p-polarized data as it is expected that these data will be less strongly influenced by coupled mode effects (12). These thickness estimates can then be refined, and linewidth and sidewall slope esti-

mates can be added by iteratively fitting using the SIE approach. Finally, these estimates can be further refined using the RCWA algorithm.

The best fits we have achieved to the near-normal incidence data are shown in Figure 5. The 75º SE data and RCWA simulation are illustrated in Figure 4. The agreement between the SEM-measured quantities and the ones from fits to optical data is good. The differences may be due to the differences between the two dies, incomplete optimization of the RCWA analysis, magnification calibration errors in the SEM, or human error in measuring the SEM photo.

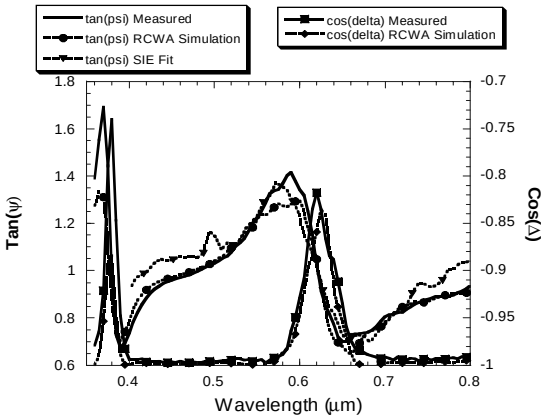

Figure 5. Near-normal (6º) SE data, SIE fit to tan(ψ) data, and RCWA simulation

The potential of SE to measure evolving grating topographies during an etch was simulated by measuring the samples etched for varying times. As can be seen in Figure 6, the basic trends in the experimental data are reflected in the modeled results. The simulations and experiments reveals similar non-monotonic behavior in both tan(Ψ) and cos(Δ) (only cos(Δ) is shown here) as the etch depth increases. By more accurately fitting theory to experimental data, it should be possible to accurate extract etch depth and wall vs. etch time from in situ data. Other RCWA simulations which we have made for 0.1 μm line/space gratings indicate that this technique will be applicable for monitoring the etching of deep submicron structures.

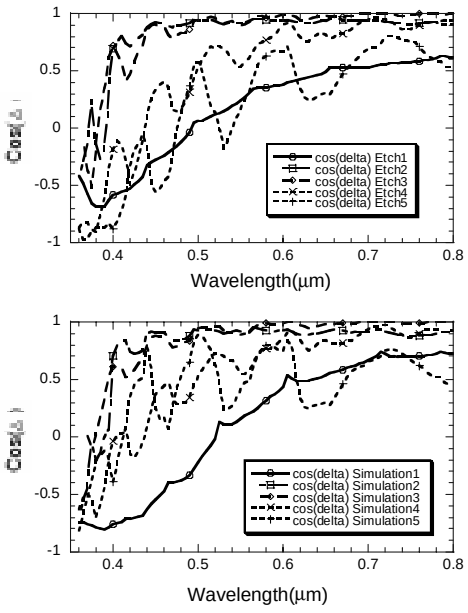

Figure 6. Comparison of simulated (upper) and experimental (lower) cos(Δ) curves at 75º angle of incidence for a series of etched 4 μm period Si gratings.

Conclusions

Use of SE and/or SR yields quantitatively accurate critical dimension and wall angle data on patterned semiconductor structures. Based on the fittings of etch data, it is possible to automate the procedure using nonlinear regression method. This is essentially an inverse problem. The ultimate goal would be to monitor geometrical parameters of wafer during deposit/etch for the purpose of processing control.

Acknowledgements

This work was supported in part by the Semiconductor Research Corporation (contract 97-FC085), AFOSR/DARPA MURI Center for Intelligent Electronics Manufacturing (AFOSR F49620-95-1-0524), and the State of Michigan Center for Display Technology and Manufacturing. The authors would also like to thank Dr. D. S. Grimard and Ms. M. Gulari for assistance with sample fabrication.

References

1. D.E. Aspnes, Solid State Communications, 101, pp.85-9 (1997)
2. T. L. Vincent, P.P. Khargonekar, and F.L. Terry, Jr., J. Electrochem. Soc., 144, pp.2467-72 (1997)
3. T. B. Benson, L.I. Kamlet, P. Klimecky, and F.L. Terry, Jr., J. Elec. Mat., 25, pp955-64 (1996)
4. H. L. Maynard, A. N. Laydi, J. T. C. Lee, J. Vac. Sci. Tech., B15, pp109-15 (1997)
5. C.J. Raymond, M.R. Murnane, S.L. Prins, S.S.H. Naqvi, J.R. McNeil, J.W. Hosch, Proc. SPIE, 2725, pp.698-709 (1996)
6. T.M. Morris, D.S. Grimard, C.F. Shu, F. L. Terry, M.E. Elta, R.C. Jain, Proc.SPIE, 1926,pp.27-32 (1993)
7. P. A. Heimann and R. J. Schutz, J. Electrochem. Soc., 131, pp. 881-5 1984).
8. Grating Solver Development Co., Allen, TX..
9. M. G. Moharam and T. K. Gaylord, J. Opt. Soc. Am., pp. 1385-1392 (1982).
10. R. Petit, ed., *Electromagnetic Theory of Gratings*, Springer-Verlag (Berlin, 1980).
11. Azzam, R.M.A. and Bashara , N.M., *Ellipsometry and Polarized Light*, Elsevier (Amsterdam, 1986).
12. D.A.Gremaux and N.C.Gallagher, Appl. Opt., 32, pp.1948-1953 (1993).